3-1-2005

# The electronic structure of oriented poly [2-methoxy-5-(2'-ethyl-hexyloxy)-1,4-phenylene-vinylene]

D.K. Chambers
*Louisiana Tech University, Institute for Micromanufacturing, Electrical Engineering Program*

S. Karanam
*Louisiana Tech University, Institute for Micromanufacturing, Electrical Engineering Program*

D. Qi
*Louisiana Tech University, Institute for Micromanufacturing, Electrical Engineering Program*

Sandra Zivanovic Selmic
*Louisiana Tech University*, sz@latech.edu

Yaroslav B. Losovyj
*Louisiana State University at Baton Rouge*, ylozovyy@indiana.edu

*See next page for additional authors*

Published in *Applied Physics A* 80 (2005), pp. 483–488. 
http://www.springerlink.com/content/1432-0630/

# The electronic structure of oriented poly [2-methoxy-5-(2'-ethyl-hexyloxy)-1,4-phenylene-vinylene]

D. K. Chambers[1], S. Karanam[1], D. Qi[1], S. Selmic[1,*], Y. B. Losovyj[2,3], L. G. Rosa[3], P. A. Dowben[3,*]

1 Louisiana Tech University, Institute for Micromanufacturing, Electrical Engineering Program, P.O. Box 10137, 911 Hergot Ave., Ruston, LA 71272, USA

2 Center for Advanced Microstructures and Devices, Louisiana State University, 6980 Jefferson Highway, Baton Rouge, LA 70806, USA

3 Department of Physics and Astronomy and the Center for Materials Research and Analysis, Behlen Laboratory of Physics, University of Nebraska–Lincoln, Lincoln, Nebraska 68588-0111, USA

*Submitted September 2004; accepted September 20, 2004; published online November 3, 2004*

**Abstract:** Poly[2-methoxy-5-(2'-ethyl-hexyloxy)-1,4-phenylene-vinylene] (MEH-PPV) adopts a preferential orientation on indium tin oxide. Although the basic building block of this polymer provides a negligible overall point-group symmetry, the polymer MEH-PPV packs with sufficient order to exhibit band structure. The polymer is fragile with bond cleavage evident following both argon-ion impact and ultraviolet radiation, but annealing leads to the restoration of much of the bond order.

## 1 Introduction

The gain in popularity of conducting polymers such as doped polyaniline (PANI) and polypyrrole, and semiconducting polymers like polythiophene and polyphenylene-vinylene (including poly[2-methoxy, 5-(2'-ethylhexyloxy)-1,4-phenylene-vinylene] or MEH-PPV), has been the promising future of organic semiconducting electroluminescent materials for electronic and opto-electronic devices. Applications in polymer light-emitting diodes (PLEDs) [1, 2], photodiodes [3], photovoltaics [4, 5], and field-effect transistors [6], among other devices, have been demonstrated for MEH-PPV. Ordered MEH-PPV samples show optical excitations that have been attributed to interband transitions [7] and electroabsorption studies have also been explained in terms of a band model [8].

The highest occupied molecular orbital (HOMO) to lowest unoccupied molecular orbital (LUMO) gap cannot always be directly compared to the effective gap in a device due to local Coulombic interactions. Nonetheless, assignments of the energy levels could help reconcile the difference of the charge transfer energy gap of > 2.35 eV [9] and the HOMO–LUMO band gap of 2.45 eV [9], observed for MEH-PPV, with the larger 2.7-eV gap that is observed [10] and calculated [11, 12] for PPV alone. The much reduced point group and much reduced local symmetry of MEH-PPV, when compared to PPV alone, must play a role [13]. We show here that local molecular orbital symmetry effects can be observed in the very low symmetry polymer MEH-PPV, and provide some indirect indications that defects must play a role in the actual device properties.

## 2 Experiment and theory

The light polarization dependent angle-resolved photoemission experiments were carried out using synchrotron radiation, dispersed by a 3-m toroidal monochromator, at the Center for Advanced Microstructures and Devices (CAMD) in Baton Rouge, Louisiana, as described elsewhere [14–16]. The measurements were performed in an ultra high vacuum (UHV) chamber employing a hemispherical electronenergy analyzer with an angular acceptance of ±1°, as described elsewhere [16]. The combined resolution of the electron-energy analyzer and monochromator varied between 0.10 and 0.25 eV. All angles (both light-incidence angles as well as photoelectron-emission angles) reported herein are with respect to the substrate surface normal. Because of the highly plane polarized nature of the dispersed synchrotron light through the toroidal grating monochromator, the large light-incidence angles result in a vector potential $\boldsymbol{A}$ more parallel to the surface normal (*p*-polarized light),while smaller light-incidence angles result in the vector potential $\boldsymbol{A}$ residing more in the plane of the surface (*s*-polarized light) in the geometry of our experiment. The dispersion of the molecular orbital bands was studied by examining the variations in the binding energies of the various photoemission features as a function of incident photon energy from 55 eV to 110 eV. For the photoemission results reported here, the photoelectrons were collected normal to the surface ($\bar{\Gamma}$ or $k_{\parallel} = 0$) to preserve the highest possible point-group symmetry and at room temperature.

Thin films of 100 nm of MEH-PPV were prepared by spin coating. Powdered MEH-PPV (Sigma Aldrich) from a single batch with molecular weight 86 000 g/mol was dissolved in chloroform. These solutions were heated to 80 °C and stirred for 8 h, then filtered and spin cast onto indium tin oxide (ITO). The MEH-PPV film thickness was mea-

*Correspondence email: sselmic@latech.edu ; pdowben@unl.edu

sured to be 90 nm with good uniformity (± 5%). These samples were then dried, in vacuo, for 8 h at room temperature.

For the transport measurements, a 100-nm Al electrode was thermally evaporated on MEH-PPV. The efficacy of the MEH-PPV films was demonstrated by fabricating photodiodes using MEH-PPV and ethyl viologen dibromide on ITO, with photocurrents, in these diodes, showing the characteristic curves of zero bias current with light exposure that is absent in the dark [17].

Damage was introduced by either synchrotron radiation, exposing the polymer to 3 h of synchrotron radiation of 65 eV, or sputtering for 3 min at $3\times10^{-6}$ Torr with 1-keV Ne ions, as discussed below.

Theoretical calculations of the electronic structure of PPV and MEH-PPV were undertaken by PM3-NDO (neglect of differential overlap) with the HyperChem package [18, 19]. The model calculations were undertaken on short chain lengths (three repeat units) that were hydrogen terminated to prevent excessive folding. Geometry optimization of the system was performed by obtaining lowest unrestricted Hartree–Fock (UHF) energy states and their possible symmetries of the polymer molecule, as indicated in Fig. 1.

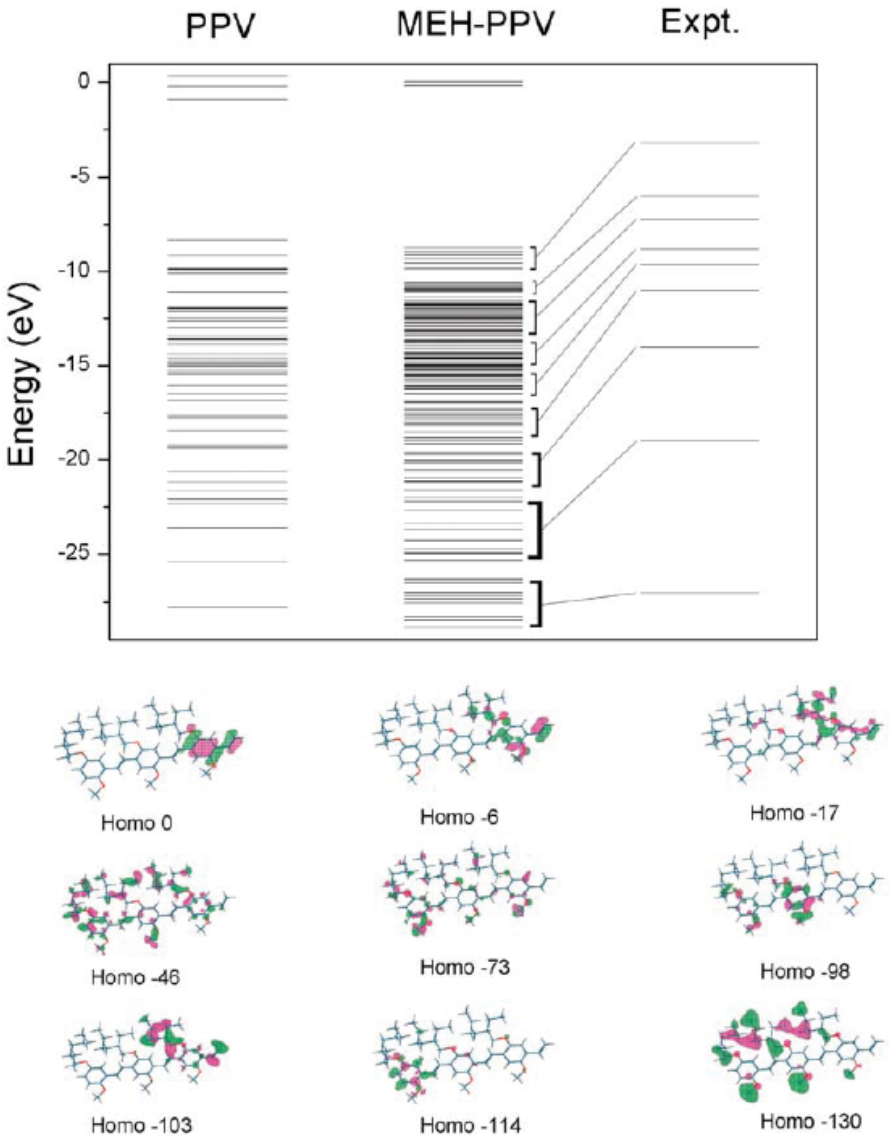


**FIGURE 1** The calculated ground state molecular orbital energies of three monomers of PPV and three monomers (repeat units) of MEH-PPV are compared with experimental binding energies with respect to the Fermi level. This includes a few unoccupied molecular orbitals down to the lowest unoccupied molecular orbital, as well as the occupied molecular orbitals referenced to the vacuum level. Selected MEH-PPV molecular orbitals (HOMO) are shown *below*, including the highest occupied molecular orbital (HOMO), HOMO-6, HOMO-17, HOMO-46, HOMO-73, HOMO-98, HOMO-103, HOMO-114, and HOMO-130. From the calculations, as shown, ground state free molecule HOMO–LUMO band gaps of 7.4 eV and 8.6 eV are derived for PPV and MEH-PPV, respectively.

### 3 Comparison between theory and experiment

In the photoemission spectra of MEH-PPV films on ITO, photoemission peaks are observed at roughly 3.3 eV and 6 eV, with overlapping features at 7.2 eV, 8.8 eV, 9.6 eV, and 11 eV, in addition to broader features at the larger binding energies of 14 eV, 19 eV, and 27 eV, as shown in Fig. 2. The occupied molecular orbitals derived from semiempirical ground state calculations can be compared to these various features observed in the photoemission (shown in Fig. 2), as has been undertaken successfully elsewhere with large molecular adsorbates [14, 15, 20–24]. Due to close placement in orbital energy of many of the different molecular orbitals as well as solid-state and lifetime broadening of the photoemission features, the individual molecular orbitals cannot be resolved in photoemission, so that several molecular orbitals contribute to a single pho-

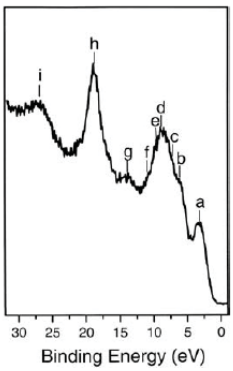


**FIGURE 2** Photoemission spectrum of MEH-PPV film on glass after reconstructive annealing with many of the features labeled for identification: (a) 3.3 eV, (b) 6 eV, (c) 7.2 eV, (d) 8.8 eV, (e) 9.6 eV, (f) 11 eV, (g) 14 eV, (h) 19 eV, and (i) 27 eV. The spectrum was taken at a photon energy of 65 eV.

toemission feature, as indicated in Fig. 1. The difference between orbital energies, obtained in theory and referenced to the vacuum level, and the experimental binding energies with respect to the Fermi level obtained for MEH-PPV from the photoemission spectra is about 4.7 eV, as indicated in Fig. 1. This shift between theory and experiment is similar to that observed for carborane films [22], fluorinated polymer films [21], and multilayer films of biphenyldiisocyanide [24] and biphenyldimethyldithiol [23] and is expected for PPV and like molecules [11].

Assuming that the chemical potential is in mid gap, the binding energy for the highest occupied molecular orbital suggests a HOMO–LUMO gap of 6 eV or more, but certainly no smaller than 3–4 eV (assuming that MEH-PPV is more of an *n*-type material, which is very unlikely). Many conducting polymers are *p*-type, including PPV [12, 25], alkoxy derivatives of PPV [26], and MEH-PPV [27, 28]. Accepting that MEH-PPV is a *p*-type semiconductor, the HOMO–LUMO gap of 8.6 eV, calculated here, for MEH-PPV and 7.4 eV for PPV are consistent with the observed photoemission data with a highest occupied molecular orbital binding energy of 3.3 eV, with respect to the Fermi level. The observed binding energy for the highest occupied molecular orbital of 3.3 eV is difficult to reconcile with the optical absorption, seen in Fig. 3, the accepted charge transfer energy gap of > 2.35 eV

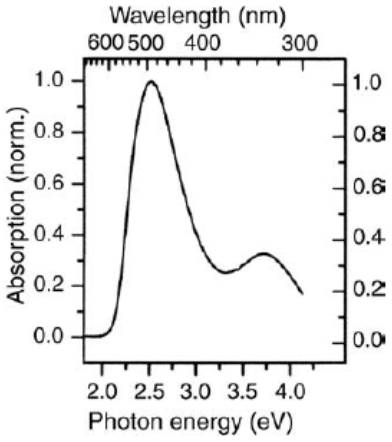


**FIGURE 3** Absorption spectrum of MEH-PPV thin film cast on quartz plate showing peak with corresponding band-gap energy of 2.5 eV.

[9], and the apparent HOMO–LUMO band gap of 2.45 eV [9], observed for MEH-PPV. Indeed, there is further qualitative disagreement with theory as PPV films have a larger (2.7-eV [10]) apparent HOMO–LUMO gap than the rough 2.5-eV gap for MEH-PPV.

The vertical peak in the optical absorption reported here (Fig. 3) is consistent with the previously reported solid state thin film HOMO–LUMO band gap of 2.45 eV [9]. While Coulomb effects that occur with optical excitation work to make this value much smaller than the HOMO–LUMO ground-state gap, the huge difference observed here must be due to defects, extrinsic carriers injected from ITO, solvent impurities, or solid-state effects (such as $\pi$–$\pi$ extramolecular interactions). The presence of the large pendant group in MEH-PPV, that is absent in PPV alone, can be anticipated to have a large influence on the extramolecular interactions in spin-coated films, but it does not appear to us that this can be the full explanation by any means.

The HOMO–LUMO gap of 8.6 eV, calculated here, for MEH-PPV and 7.4 eV for PPV, while consistent with the photoemission, are very different from the 2 eV [12] and 2.5 eV [11] gaps calculated for PPV. Indeed, our values for the HOMO–LUMO gap are consistent with the calculated band structure only in the vicinity of the Brillouin-zone center ($\Gamma$) and along some high symmetry directions of the PPV crystal, where a direct band gap of about 7 eV is indicated [12]. Since we have taken our photoemission spectra for the normal emission, it may be that we do not probe the smaller band gap seen at the Brillouin-zone edge in our measurements. Given that there is significant band dispersion in crystalline MEH-PPV and PPV, as discussed below, this difference between the measured optical gap and the photoemission strongly suggests that solid-state effects play some (but probably not an exclusive) role in determining the optical band gap. It may be that a correlation energy may be ultimately indicated as a necessary addition to an LDA or DFT solid-state calculation.

Increasing the chain length does not decrease the calculated HOMO–LUMO

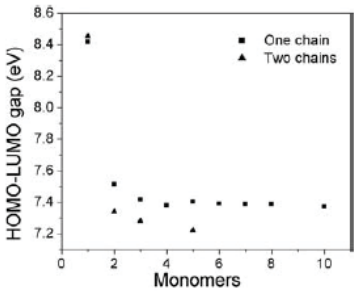


**FIGURE 4** The HOMO–LUMO gap abstracted from the calculated ground state molecular orbital energies of PPV for an increasing number of monomers (repeat units) of PPV. A single chain is compared with a double chain of PPV.

gap significantly after three units (a polymer with three or more repeat units) are reached, as shown for a single chain and a double chain of PPV in Fig. 4. It is significant that the calculated HOMO–LUMO gap does decrease by increasing the number of chains.

## 4 Molecular orientational order and band structure

We see strong light-polarization effects in the photoemission spectra of MEH-PPV on ITO by changing the light-incidence angle from a large incidence angle (a vector potential $\boldsymbol{A}$ more parallel to the surface normal or *p*-polarized light) to a smaller incidence angle (with the vector potential $\boldsymbol{A}$ residing more in the plane of the surface or *s*+ *p*-polarized light) in the geometry of our experiment. This comparison of light incidence angle photoemission spectra, with the photoelec-

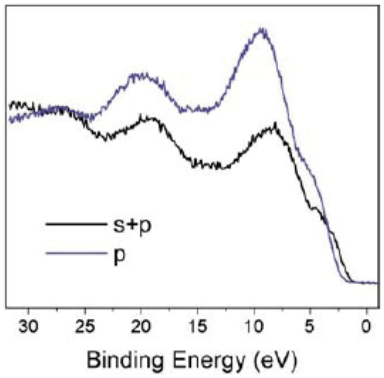


**FIGURE 5** MEH-PPV photoemission spectra comparing *s*+ *p* versus *p* polarizations of the incident light. The spectra were taken at a photon energy of 60 eV and the photoelectrons collected at normal emission.

trons being collected along the normal to the surface ($\bar{\Gamma}$), is shown in Fig. 5.

Although MEH-PPV is a very low symmetry polymer, by considering the application of symmetry-selection rules to the light polarization dependent photoemission (Fig. 5), some insight into the preferential orientation may be obtained. As is typical with large organic molecules [20], the partial cross section for photoemission varies according to the orientation of the light vector potential $\boldsymbol{A}$ and the symmetry of the initial state $\Psi_i$ and, assuming that the final state wave function $\Psi_f$ (for electrons collected along the surface normal) is fully symmetric, according to

$$\left(\frac{\mathrm{d}\sigma}{\mathrm{d}\Omega}\right)_{\mathrm{PES}} \propto \left|\langle\Psi_f|\, \boldsymbol{A}\bullet\mathbf{p}+\mathbf{p}\bullet\boldsymbol{A}\,|\Psi_i\rangle\right|^2 \times \delta(E_f-E_i-h\upsilon)\,. \quad (1)$$

The evidence of strong light-polarization effects suggests a strong preferential orientation of the polymer chains, as has been observed in other polymer systems [15, 20], including a number of conducting polymers like polyaniline and polypyrrole [15]. Unfortunately, because the symmetry of MEH-PPV is so very low, and because of the huge number of overlapping molecular orbitals that contribute to each photoemission feature, we cannot ascertain, from Fig. 5, the preferential orientation adopted by MEH-PPV in our films.

There is further evidence of strong preferential order adopted by the MEH-PPV molecular chains in our films. A sequence of photon energy dependent photoemission spectra were taken for thin films of MEH-PPV, as shown in Fig. 6. The MEH-PPV photoemission peaks c, e, g, and h, as labeled in Fig. 1, exhibit small shifts in binding energy as a function of photon energy. Because the photoelectrons are collected along the surface normal in the sequence of photon energy dependent photoemission spectra, the binding energy shifts of many of the observed photoemission features are indicative of band dispersion along the electron wave vector normal to the surface, $k_\perp$. The value of $k_\perp$ can be estimated from the photoelectron kinetic energy making some assumptions about the inner potential $U_{\mathrm{in}}$:

$$k_\perp = \sqrt{\frac{2m}{\hbar^2}\left\{E_{\mathrm{kin}}\,(\cos(\theta))^2 + U_{\mathrm{in}}\right\}}\,. \quad (2)$$

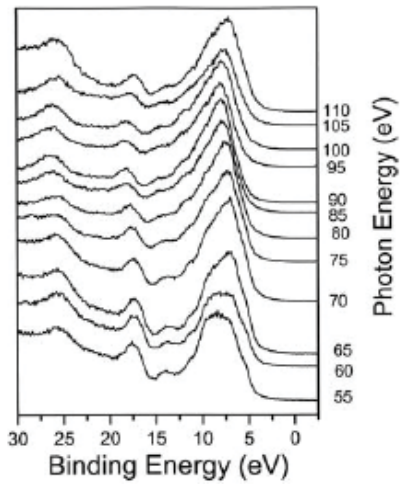


**FIGURE 6** Photoemission spectra of MEH-PPV thin film as a function of incident photon energy. Shifts in binding energy peaks indicate band dispersion along $k_\perp$ in bulk material. The photoelectrons were collected at normal emission.

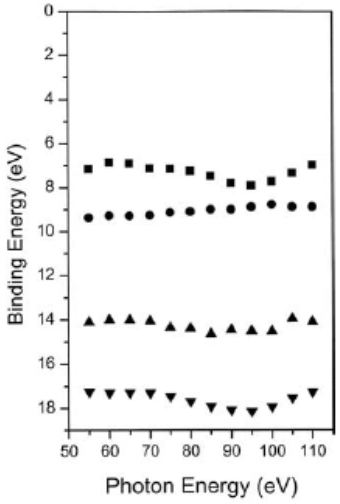


**FIGURE 7** Plot of spectral peak dispersion as a function of incident photon energy for several photoemission features at different binding energies, abstracted from Fig. 5. These data suggest molecular orbital periodicity in bulk material normal to the MEH-PPV thin-film surface, and the existence of band structure (see text).

The dispersion of the molecular orbitals, summarized in Fig. 7, shows band critical point repetition, suggesting periodicity of about 4.13 Å perpendicular to the film or along the surface normal, and has been observed with other ordered large-molecule films [20, 21, 23]. Such band structure, whether intramolecular or extramolecular, is also indicative of strong preferential ordering of the polymer chains. For this reason, we cannot ascribe the small HOMO–LUMO gap of the MEH-PPV device structures to orientational disorder. Solid-state effects and other extrinsic effects must now be expected to play a role if such order is preserved in the MEH-PPV device structures, as noted above.

Qualitatively, based on the band structure calculated for PPV [11, 12], the band dispersions observed here are expected. Our band dispersions here seem to be of the order of 1 eV, which is much smaller than the calculated band widths of 2.8 eV [11] and band dispersions of 4 eV [12] calculated for PPV. Because the photoemission features contain many overlapping molecular orbitals, and we do not precisely know the structure and orientation of MEH-PPV in our films, we cannot ascertain the origin of the smaller than expected band dispersion observed here. Density functional theory (DFT) and local density approximation (LDA) calculations are known to have problems obtaining the correct band gap in inorganic semiconductors, particularly near the Brillouin-zone edge, adding further complications to the analysis.

The evidence does, nonetheless, point to a very high degree of ordering in these spin-cast films. This is somewhat surprising because pendant groups attached to long-chain molecules are usually associated with disorder (e.g. [29]), but there are many cases where the pendent groups order [30, 31]. Disorder has been attributed to a decrease in hole mobility in PPV [25] and MEH-PPV [27, 32], but annealing and preparation methods can substantially affect order [32–34]. Pendant groups [32] rather than the torsion angle of the polymer backbone [25] are implicated as the origin of disorder in MEH-PPV, consistent with the photoemission results reported here.

## 5 The role of defects

In order to understand the role of defects, we have purposely introduced defects into the MEH-PPV films by Ne-ion sputtering at 1 keV. The Ne ions, we believe, introduce a significant number of defects, as is indicated by the increased widths of the photoemission features.

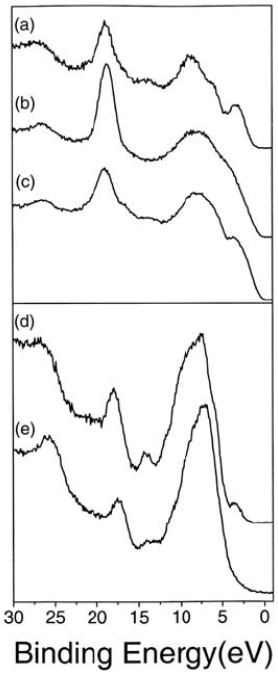


**FIGURE 8** Photoemission spectra of annealed MEH-PPV film (a) before and (b) after 1-keV Ne-ion sputtering and again (c) after re-annealing to 90 ◦C. Similar diminution of spectral peak features is seen in annealed MEH-PPV thin films (d) before and (e) after a 3-h ultraviolet exposure to 65-eV synchrotron radiation.

The effect of these defects on MEH-PPV valence-band electronic structure is seen in Fig. 8, by comparing an annealed MEH-PPV film before (a) and after (b) Ne-ion sputtering. Of key importance is not only the increasingly broad photoemission features, but also the density of states that begins to trail to smaller binding energies in the vicinity of the Fermi level. These defects, whose nature we cannot determine from our measurements here, do much to close the effective HOMO–LUMO gap.

It is also interesting to note that again annealing the film after the damage is introduced into the film by Ne-ion sputtering appears to 'repair' some of the damage. In Fig. 8c, we show the photoemission spectra after re-annealing the MEH-PPV film to 90 °C. After the damaged film is re-annealed, the photoemission feature widths decrease and many of the photoemission features can again be identified. It is doubtful that this damaged and again annealed film is restored to the original condition of the film annealed in vacuo, but some of the effects of damage are reversed. The restoration and improvement of the molecular order has been observed in mobility measurements [32–34] as a consequence of annealing treatments of the film, but defect reduction, as a result of annealing treatments, may have also occurred in those studies.

A similar effect is observed after long exposures of the MEH-PPV films to vacuum ultraviolet light (65-eV photon energy for 3 h). This is evident when comparing an MEH-PPV film before (Fig. 8d) and after (Fig. 8e) 3 h of vacuum ultraviolet light exposure. Peaks a, b, g, and i, as identified in Fig. 2, can no longer be identified following this harsh treatment. Ultraviolet light is known to cause damage to large organic polymers [35–37], largely through bond cleavage, and there is reason to expect MEH-PPV to be less robust than many of these species.

Defects are believed to contribute to the density of localized carriers [12], consistent with our studies here. Nonetheless, even our highly ordered polymer films, made with a high molecular weight species, may contain a considerable number of defects [25]. Such defects could significantly contribute to a smaller apparent optical gap, but would not be observed in photoemission.

## 6 Summary

Polymer MEH-PPV films spin coated on indium tin oxide exhibit a high degree of preferential molecular order. The electronic structure appears to be in good agreement with the predictions obtained from semi-empirical molecular orbital calculations. Nonetheless, it is clear that defects (bond cleavage), solid-state effects, and extrinsic effects may play a role in the performance of an organic device that includes MEH-PPV as a component. With the high level of order, it is clear that the molecular orbitals do contribute to dispersing bands, much like those seen in inorganic semiconductors.

**ACKNOWLEDGEMENTS**

This work was supported by the National Science Foundation through Grant No. CHE-0415421 and the NSF 'QSPINS' MRSEC (DMR-0213808), as well as by the Louisiana Board of Regents through the Board of Regents Support Fund under Contract No. LEQSF (2003–2006)-RD-A-18. We thank Dr. Y. Lvov for his assistance in this work.

**REFERENCES**

1 D. Braun, A. Heeger: Appl. Phys. Lett. **58**, 1982 (1991)
2 S.A. Carter, J.C. Scott, P.J. Brock: Appl. Phys. Lett. **71**, 1145 (1997)
3 J.J.M. Halls, C.A. Walsh, N.C. Greenham, E.A. Marseglia, R.H. Friend, S.C. Moratti, A.B. Holmes: Nature **376**, 498 (1995)
4 G. Yu, J. Gao, J.C. Hummelen, F. Wudl, A.J. Heeger: Science **270**, 1789 (1995)
5 M. Granstrøm, K. Petritisch, A.C. Arias, A. Lux, M.R. Andersson, R.H. Friend: Nature **395**, 257 (1998)
6 R.J.O.M. Hoofman, M.P. de Haas, L.D.A. Siebbels, J.M. Warman: Nature **392**, 54 (1998)
7 T.W.Hagler, K. Pakbaz, K. Voss, A.J. Heeger: Phys. Rev. B **44**, 8652 (1991)
8 I.D. Parker: J. Appl. Phys. **75**, 1658 (1993)
9 I.H. Campbell, T.W. Hagler, D.L. Smith, J.P. Ferraris: Phys. Rev. Lett. **76**, 1900 (1996)
10 M. Onoda, Y. Manda, T. Iwasa, H. Nakayama, K. Amakawa: Phys. Rev. B **42**, 11 826 (1990)
11 J.L. Brédas, R.R. Chance, R.H. Baughman: J. Chem. Phys. **76**, 3673 (1982)
12 P. Gomes da Costa, R.G. Dandrea, E.M. Conwell: Phys. Rev. B **47**, 1800 (1993)
13 J.M. Leng, S. Jeglinski, X. Wei, R.E. Benner, Z.V. Vardeny: Phys. Rev. Lett. **72**, 156 (1994)
14 A.N. Caruso, R. Rajesh, G. Gallup, J. Redepenning, P.A. Dowben: J. Phys.: Condens. Matter **16**, 845 (2004)
15 J. Choi, M. Chipara, B. Xu, C.S. Yang, B. Doudin, P.A. Dowben: Chem. Phys. Lett. **343**, 193 (2001)
16 P.A. Dowben, D. LaGraffe, M. Onellion: J. Phys.: Condens. Matter **1**, 6571 (1989)
17 D. Qi, K. Varahramyan, S. Selmic: MRS Symp. Proc. **814**, I11.7.1 (2004)
18 J.J.P. Stewart: J. Comput. Chem. **10**, 209 (1989)
19 J.J.P. Stewart: J. Comput. Chem. **10**, 221 (1989)
20 P.A. Dowben, J. Choi, E. Morikawa, B. Xu: 'The Band Structure and Orientation of Molecular Adsorbates on Surfaces by Angle-Resolved Electron Spectroscopies.' In: *Handbook of Thin Films, Vol. 2, Characterization and Spectroscopy of Thin Films*, ed. by H.S. Nalwa (Academic Press, New York 2002) Chap. 2, pp. 61–114
21 C.-G. Duan, W.N. Mei, J.R. Hardy, S. Ducharme, J. Choi, P.A. Dowben: Europhys. Lett. **61**, 81 (2003)

22 A.N. Caruso, L. Bernard, B. Xu, P.A. Dowben: J. Phys. Chem. B **107**, 9620 (2003)

23 A.N. Caruso, R. Rajesekaran, G. Gallup, J. Redepenning, P.A. Dowben: J. Phys.: Condens. Matter **16**, 845 (2004)

24 A.N. Caruso, R. Rajesh, G. Gallup, J. Redepenning, P.A. Dowben: J. Phys. Chem. B **108**, 6910 (2004)

25 F.C. Grozema, P.T. van Duijnen, Y.A. Berlin, M.A. Ratner, L.D.A. Siebbeles: J. Phys. Chem. B **106**, 7791 (2002)

26 G. Hadziioannou, P.F. van Hutten (Eds.): *Semiconducting Polymers* (Wiley-VCH, Weinheim 2000) p. 11

27 L. Bozano, S.A. Carter, J.C. Scott, G.G. Malliaras, P.J. Brock: Appl. Phys. Lett. **74**, 1132 (1999)

28 P.W.M. Blom, M.J.M. de Jong, S. Breedijk: Appl. Phys. Lett. **71**, 930 (1997)

29 E. Morikawa, V. Saile, K.K. Okudaira, Y. Azuma, K. Meguro, Y. Harada, K. Seki, S. Hasegawa, N. Ueno: J. Chem. Phys. **112**, 10 476 (2000)

30 K.K. Okudaira, E. Morikawa, S. Hasegawa, H. Ishii, Y. Azuma, M. Imamura, H. Shimada, K. Seki, N. Ueno: Nucl. Instrum. Methods A **467**, 1233 (2001)

31 K.K. Okudaira, E. Morikawa, D.A. Hite, S. Hasegawa, H. Ishii, M. Imamura, H. Shimada, Y. Azuma, K. Meguro, Y. Harada, V. Saile, K. Seki, N. Ueno: J. Electron Spectrosc. Relat. Phenom. **103** [Spec. Issue], 389 (1999)

32 A.R. Inigo, H.-C. Chiu, W. Fann, Y.-S. Hwang, U.-Ser Jeng, T.-L. Lin, C.-H. Hsu, K.-Y. Peng, S.-A. Chen: Phys. Rev. B **69**, 075 201 (2004)

33 G.H. Gelinck, J.M. Warman: J. Phys. Chem. **100**, 20 035 (1996)

34 G.H. Gelinck, J.M. Warman, H.F.M. Schoo: J. Radioanal. Nucl. Chem. **232**, 115 (1998)

35 M. Ono, E. Morikawa: J. Phys. Chem. B **108**, 1894 (2004)

36 E. Morikawa, J.W. Choi, H.M. Manohara, H. Ishii, K. Seki, K.K. Okudaira, N. Ueno: J. Appl. Phys. **87**, 4010 (2000)

37 J.W. Choi, H.M. Manohara, E. Morikawa, P.T. Sprunger, P.A. Dowben, S.P. Palto: Appl. Phys. Lett. **76**, 381 (2000)